The Interaction of APOBEC3G with Human Immunodeficiency Virus Type 1 Nucleocapsid Inhibits tRNA$_3^{\mathrm{Lys}}$ Annealing to Viral RNA[▽]

Fei Guo,[1] Shan Cen,[1,2] Meijuan Niu,[1] Yiliang Yang,[1] Robert J. Gorelick,[4] and Lawrence Kleiman[1,2,3]*

Lady Davis Institute for Medical Research and McGill AIDS Centre, Jewish General Hospital,[1] and Departments of Medicine[2] and Microbiology & Immunology,[3] McGill University, Montreal, Quebec, Canada H3T 1E2, and AIDS Vaccine Program, Basic Research Program, SAIC-Frederick, Inc., NCI-Frederick, Frederick, Maryland 21702[4]

Human immunodeficiency virus type 1 (HIV-1) containing human APOBEC3G (hA3G) has a reduced ability to produce viral DNA in newly infected cells. At least part of this hA3G-facilitated inhibition is due to a cytidine deamination-independent reduction in the ability to initiate reverse transcription. HIV-1 nucleocapsid (NCp7) is required both for the incorporation of hA3G into virions and for the annealing between viral RNA and tRNA$_3^{\mathrm{Lys}}$, the primer tRNA for reverse transcription. Herein we present evidence that the interaction of hA3G with nucleocapsid is required for the inhibition of reverse transcription initiation. A tRNA$_3^{\mathrm{Lys}}$ priming complex was produced in vitro by the NCp7-facilitated annealing of tRNA$_3^{\mathrm{Lys}}$ to synthetic viral RNA in the absence or presence of hA3G. The effect of hA3G on the annealing of tRNA$_3^{\mathrm{Lys}}$ to viral RNA and the ability of tRNA$_3^{\mathrm{Lys}}$ to initiate reverse transcription was measured. Our results show the following. (i) Electrophoretic band shift and primer binding site assays show that hA3G reduces the annealing of tRNA$_3^{\mathrm{Lys}}$ 44 and 60%, respectively, but does not disrupt the annealed complex once formed. (ii) hA3G inhibits tRNA$_3^{\mathrm{Lys}}$ priming 70 to 80%. (iii) Inhibition of tRNA$_3^{\mathrm{Lys}}$ priming by hA3G requires an interaction between hA3G and NCp7 during annealing. Thus, annealing of tRNA$_3^{\mathrm{Lys}}$ is insensitive to hA3G inhibition when facilitated by a zinc finger mutant of NCp7 unable to interact with hA3G. NCp7-independent annealing of DNA to viral RNA also is insensitive to hA3G inhibition. These results indicate that hA3G does not sterically block tRNA$_3^{\mathrm{Lys}}$ annealing by binding to viral RNA. Annealing and priming are not affected by another RNA binding protein, QKI-6.

During human immunodeficiency virus type 1 (HIV-1) assembly, tRNA$^{\mathrm{Lys}}$ (composed primarily of tRNA$_{1,2}^{\mathrm{Lys}}$ and tRNA$_3^{\mathrm{Lys}}$) is selectively packaged into the virion, and tRNA$_3^{\mathrm{Lys}}$ is annealed to the primer binding site (PBS) and sequences upstream of the PBS in the 5′ region of the viral RNA genome (for a review, see reference 32). After introduction of the HIV-1 RNA genome into a newly infected cell, the initiation of viral DNA synthesis by reverse transcriptase (RT) is primed by the tRNA$_3^{\mathrm{Lys}}$. The annealing of tRNA$_3^{\mathrm{Lys}}$ to viral RNA is facilitated both by nucleocapsid sequences in Gag (9, 15) and by mature nucleocapsid NCp7 (13, 33), and it has been reported that the annealing of tRNA$_3^{\mathrm{Lys}}$ to viral RNA by Gag requires exposure to mature NCp7 to achieve a configuration required for optimal initiation of reverse transcription (10). Annealing of tRNA$_3^{\mathrm{Lys}}$ to viral RNA does not appear to require the zinc fingers in nucleocapsid, but it does require the basic amino acids flanking the first zinc finger (9, 13, 22, 33).

In certain cell types, termed nonpermissive, including the main target cells of HIV-1, T lymphocytes and macrophages, HIV-1 will replicate efficiently only in the presence of the viral protein Vif (16, 17, 45). These cells produce the protein human APOBEC3G (hA3G), the presence of which can inhibit viral replication (38, 43). Vif can prevent incorporation of hA3G into viruses (30) by binding to it in the cytoplasm (39) and targeting it for proteosomal degradation (44, 48). Vif-negative

HIV-1 produced in nonpermissive cells contains hA3G, and infection in new cells is accompanied by a strong reduction in the overall production of new viral DNA (18, 36, 39). Estimates of the reduction in production of minus-strand strong-stop DNA have varied from 50 to 84% (18, 37, 38, 40), and we have reported 55 and 95% reductions in the production of minus-strand strong-stop DNA and late DNA, respectively (19).

The minus-strand DNA that is made in the presence of hA3G contains 1 to 2% cytosines mutated to uracil (23, 35, 38, 51). Because hA3G is a cytidine deaminase (38, 47, 51), it has been suggested that the decreased production in viral DNA results from the hA3G-facilitated cytidine deamination of viral DNA, followed by its degradation by enzymes of the DNA repair system, but evidence for this remains inconclusive (29). In fact, a number of reports have shown that mutant hA3G lacking cytidine deaminase activity still has a strong inhibitory effect on HIV-1 replication (4, 23, 41). We have recently reported that the in vivo inhibition of minus-strand strong-stop DNA production by hA3G can occur independently of cytidine deamination, and that the reduction in DNA production is correlated with a similar reduction in the ability to initiate reverse transcription (19).

The incorporation of hA3G into HIV-1 requires nucleocapsid sequences in Gag (1, 8, 31, 42, 50). This incorporation appears to require RNA (31, 42, 50) but not specifically viral genomic RNA. Since both hA3G and nucleocapsid are RNA binding proteins, it has been proposed either that the nucleocapsid domain in Gag interacts with hA3G via an RNA bridge or that RNA binding to either protein produces conformational changes allowing the proteins to interact. The former

* Corresponding author. Mailing address: Lady Davis Institute for Medical Research, Jewish General Hospital, 3755 Cote St. Catherine Rd., Montreal, Quebec, Canada H3T 1E2. Phone: (514) 340-8260. Fax: (514) 340-7502. E-mail: lawrence.kleiman@mcgill.ca.

hypothesis predicts that Gag and hA3G bind nonspecifically to cellular RNAs and that Gag, through an RNA bridge, carries hA3G into the virion. However, the fact that the RNA bridge hypothesis does not easily explain why the mouse form of A3G is not incorporated into murine virions but is incorporated into HIV-1 makes the role of RNA in altering protein conformation to allow interaction a more attractive hypothesis (12, 49).

In this report, we show that hA3G inhibits both $tRNA_3^{Lys}$ annealing and initiation of reverse transcription in a simple in vitro system in which $tRNA_3^{Lys}$ is annealed to viral RNA with NCp7 in the absence or presence of hA3G. The inhibition depends on an RNA-facilitated interaction between NCp7 and hA3G that occurs during the annealing process.

MATERIALS AND METHODS

Protein production. hA3G was produced in baculovirus using the Baculo expression system and was purified by $(NH_4)_2SO_4$ fractionation and immunoaffinity chromatography to >95% purity (Diagnostics, Inc.). HIV-1 RT was purified from bacteria as previously described (24). Recombinant purified wild-type and mutant NCp7 were prepared as previously described (7, 20), including purification by reverse-phase high-pressure liquid chromatography after denaturing the protein in 8 M guanidine hydrochloride. QKI-6 RNA binding protein was a gift from Stephane Richard (McGill University).

In vitro annealing of $tRNA_3^{Lys}$ to viral RNA. $tRNA_3^{Lys}$ was purified from human placenta, as previously described (28), using standard chromatography procedures (sequentially, DEAE-Sephadex A-50, reverse-phase chromatography [RPC-5], and Porex C4) and two-dimensional polyacrylamide gel electrophoresis (2D PAGE). Synthetic HIV-1 genomic RNA was synthesized as previously described (24) from the AccI-linearized plasmid HIV-PBS (2) with the MEGA-script transcription system (Ambion, Inc.). The synthetic genomic RNA comprises the complete R and U5 regions, the PBS, the leader, and part of the *gag* coding region. For heat annealing, 1 pmol of $tRNA_3^{Lys}$ was combined with 1 pmol of synthetic HIV-1 RNA template in a solution containing 50 mM Tris-HCl (pH 7.5), 60 mM KCl, 3 mM $MgCl_2$, 10 mM dithiothreitol (DTT), and 10 U of RNasin. The annealing reaction mixture was heated sequentially at 85°C for 5 min, at 50°C for 10 min, and then at 37°C for 15 min. For NCp7-facilitated annealing, 1 pmol of $tRNA_3^{Lys}$ was annealed to 1 pmol of synthetic HIV-1 RNA template by incubating these reagents at 37°C for 90 min with 30 pmol of NCp7 in a 10-μl reaction mixture containing 50 mM Tris-HCl (pH 7.2), 50 mM KCl, 5 mM $MgCl_2$, 10 mM DTT, and 10 U of RNasin. To study the effect of APOBEC3G on this annealing, 1 pmol of either purified APOBEC3G or control bovine serum albumin (BSA), dissolved in 20 mM Tris-HCl (pH 7.5), 0.1 M NaCl, and 0.01% sarcosyl, was added to the annealing reaction mixtures at the start. After the annealing, the $tRNA_3^{Lys}$/viral RNA complex was deproteinized through the addition of 1 μl proteinase K (5 mg/ml) and was incubated at 37°C for 30 min, followed by phenol-chloroform extraction and alcohol precipitation of the viral RNA complex.

Measurement of $tRNA_3^{Lys}$ or DNA annealing to viral RNA. (i) Electrophoretic mobility shift assay. $tRNA_3^{Lys}$ was 3′ end labeled with [^{32}P]pCp, as previously described (6). For measuring the annealing of an 18-nucleotide (nt) DNA primer (5′-GTCCCTGTTCGGGCGCCA-3′) that is complementary to the PBS, the DNA was 5′ end labeled with ^{32}P using T4 kinase (Invitrogen). After deproteinization of the annealed complex with proteinase K, the free $tRNA_3^{Lys}$ or DNA oligomer was resolved from primer complexed with viral RNA using one-dimensional (1D) 6% PAGE.

(ii) $tRNA_3^{Lys}$ occupation of the PBS. A 21-nt DNA oligomer (5′-GAGTCCT GCGTCGAGAGAGCT-3′) was 5′ end labeled with ^{32}P using T4 kinase and was annealed to complementary sequences in the $tRNA_3^{Lys}$/viral RNA complex 25 bases downstream of the PBS. The complex was then incubated at 37°C for 30 min in 20 μl of RT buffer (50 mM Tris-HCl [pH 7.5], 60 mM KCl, 3 mM $MgCl_2$, and 10 mM DTT) containing 50 ng of purified HIV RT, 10 U of RNasin, 200 μM deoxynucleoside triphosphates, and reaction products, either full length (226 nt) or truncated (46 nt, due to occupation of the PBS by $tRNA_3^{Lys}$), were resolved using 1D 6% PAGE with gels containing 7 M urea.

$tRNA_3^{Lys}$ priming of reverse transcription. $tRNA_3^{Lys}$ annealed to viral genomic RNA was used to measure the $tRNA_3^{Lys}$ priming in an in vitro reverse transcription system, as previously described (19). After the annealing and in preparation for the $tRNA_3^{Lys}$ priming reaction, the $tRNA_3^{Lys}$/viral RNA complex was deproteinized through the addition of 1 μl proteinase K (5 mg/ml) and was incubated

at 37°C for 30 min, following which both proteinase K and digested residual proteins were phenol-chloroform extracted and the RNA was ethanol precipitated. The RNA complex was incubated at 37°C for 15 min in 20 μl of RT buffer (50 mM Tris-HCl [pH 7.5], 60 mM KCl, 3 mM $MgCl_2$, and 10 mM DTT) containing 50 ng of purified HIV RT, 10 U of RNasin, and various deoxynucleoside triphosphates. To measure the ability of annealed $tRNA_3^{Lys}$ to be extended by six deoxyribonucleotides, the RT reaction mixture contained 200 μM dCTP, 200 μM dTTP, 5 μCi of [α-^{32}P]dGTP, and 50 μM ddATP. Reaction products were resolved using 1D 6% PAGE in gels containing 7 M urea.

In vitro detection of the NCp7-hA3G interaction. Equimolar amounts of NCp7 and APOBEC3G were mixed for 2 h at 4°C in NET-gelatin buffer (50 mM Tris-HCl [pH 7.5], 150 mM NaCl, 0.1% NP-40, and 0.25% gelatin). APOBEC3G was then immunoprecipitated from the mixture by incubation with anti-APOBEC3G rabbit antiserum (NIH AIDS Research and Reference Reagent Program) at 4°C overnight. Protein A-Sepharose CL-4B beads (Amersham Pharmacia Biotech) were added to the antibody-containing samples, and the samples were incubated for a further 1 h at 4°C to allow the beads to bind to the antibody-antigen complexes. The beads were washed three times with NET-gelatin buffer containing 1% Triton X-100, and the bound proteins were heated in gel loading buffer and resolved by 1D sodium dodecyl sulfate (SDS)-PAGE. For the RNase A treatment, 100 μg of RNase A was added separately to both NCp7 and APOBEC3G before mixing the two, or 200 μg of RNase A was added to the reaction mixture after a 2-h incubation at 4°C and then was incubated at 37°C for 15 min.

Western blot analysis. Protein samples were separated by SDS-15% PAGE, followed by blotting onto nitrocellulose membranes (Gelman Science). Western blots were probed with either rabbit anti-APOBEC3G (1:5,000 dilution) (NIH AIDS Research and Reference Reagent Program) or goat anti-NCp7 (1:5,000 dilution; goat no. 77) (a gift from Louis Henderson from the AIDS Vaccine Program). Horseradish peroxidase-conjugated secondary antibodies used were either anti-rabbit immunoglobulin (1:5,000 dilution) (Amersham Pharmacia Biotech) or anti-goat immunoglobulin (1:5,000 dilution) (Rockland Immunochemicals). Protein bands were detected by enhanced chemiluminescence (Perkin-Elmer Life Science, Inc). Bands in Western blots were quantitated using ImageJ 1.35s public domain software (NIH).

RESULTS

Inhibition of $tRNA_3^{Lys}$ priming of reverse transcription by hA3G. Synthetic viral genomic RNA (1 pmol), $tRNA_3^{Lys}$ isolated from human placenta (1 pmol), and different amounts of wild-type NCp7 were mixed together as described in Materials and Methods. The resulting $tRNA_3^{Lys}$/viral RNA complex, with NCp7 or deproteinized, was then used as a source of primer $tRNA_3^{Lys}$/template viral RNA in an in vitro reverse transcription system containing HIV-1 RT and deoxynucleotides. The first six deoxynucleotides added to the 3′ terminus of $tRNA_3^{Lys}$ during the initiation of reverse transcription are in the order 5′CTGCTA3′. Figure 1A shows the radioactive $tRNA_3^{Lys}$ extended by 6 bases in the presence of dCTP, dTTP, 5 μCi of [α-^{32}P]dGTP, and ddATP and resolved by 1D PAGE. There is also a slower-moving tRNA extension product that may represent misincorporation at position 6 rather than ddATP, which will result in ddATP being incorporated at a later position in the DNA. Lanes a to c represent reactions in which increased concentrations of NCp7 were used to anneal the $tRNA_3^{Lys}$ to the viral genome. In addition, lanes a to c represent reverse transcription reaction mixes that still contain the NCp7 used for annealing. Lanes d and e also represent annealing reactions using increased concentrations of NCp7, but in this case, the primer/template RNA complex used had been deproteinized prior to use in the RT system using, sequentially, protease K, phenol-chloroform extraction, and then alcohol precipitation of the RNA. These data show that annealing is increased with increased amounts of NCp7 used and that the presence of NCp7 in the RT reaction mix results in much less
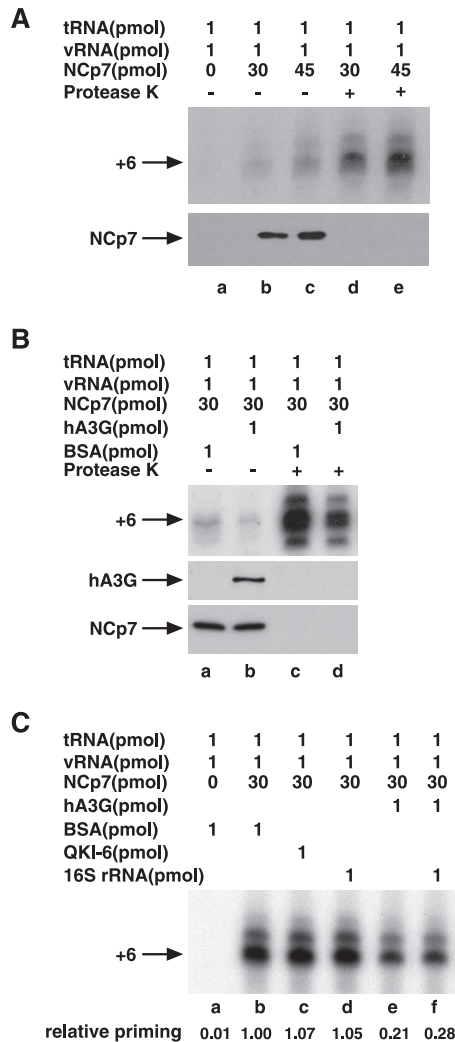
A

tRNA(pmol)	1	1	1	1	1
vRNA(pmol)	1	1	1	1	1
NCp7(pmol)	0	30	45	30	45
Protease K	-	-	-	+	+

+6 →

NCp7 →

a b c d e

B

tRNA(pmol)	1	1	1	1
vRNA(pmol)	1	1	1	1
NCp7(pmol)	30	30	30	30
hA3G(pmol)		1		1
BSA(pmol)	1		1	
Protease K	-	-	+	+

+6 →

hA3G →

NCp7 →

a b c d

C

tRNA(pmol)	1	1	1	1	1	1
vRNA(pmol)	1	1	1	1	1	1
NCp7(pmol)	0	30	30	30	30	30
hA3G(pmol)					1	1
BSA(pmol)	1	1				
QKI-6(pmol)			1			
16S rRNA(pmol)				1		1

+6 →

a b c d e f

relative priming 0.01 1.00 1.07 1.05 0.21 0.28

FIG. 1. Inhibition of NCp7-facilitated tRNA$_3^{Lys}$ priming of reverse transcription by hA3G. Synthetic viral genomic RNA and purified human placental tRNA$_3^{Lys}$ were incubated with NCp7 as described in Materials and Methods. The resulting tRNA$_3^{Lys}$/viral RNA (vRNA) complex (annealed complex), either with the NCp7 used for annealing or deproteinized, was then used as a source of primer tRNA$_3^{Lys}$/template viral genomic RNA in an in vitro reverse transcription system containing HIV-1 RT and deoxynucleotides. (A) The upper portion shows 1D PAGE patterns of tRNA$_3^{Lys}$ extended by 6 bases in the presence of dCTP, dTTP, 5 μCi of [α-^{32}P]dGTP, and ddATP, as described in Materials and Methods. Lanes a to c, tRNA$_3^{Lys}$ priming carried out in the presence of the NCp7 used for the annealing; d and e, tRNA$_3^{Lys}$ priming carried out using deproteinized tRNA$_3^{Lys}$/viral RNA annealed complex. The lower portion shows Western blots of end reactions probed with anti-NCp7. (B) The upper portion shows 1D PAGE patterns of tRNA$_3^{Lys}$ extended by 6 bases. The effect of hA3G upon tRNA$_3^{Lys}$ priming is shown. During formation of the annealed complex, either hA3G or BSA was added. Lanes a and b, tRNA$_3^{Lys}$ priming carried out using an annealed complex not deproteinized; c and d, tRNA$_3^{Lys}$ priming carried out using a deproteinized annealed complex. The middle and lower portions show Western blots of end reactions probed with either anti-hA3G or anti-NCp7. (C) 1D PAGE patterns of tRNA$_3^{Lys}$ extended by 6 bases. The specificity of hA3G inhibition of tRNA$_3^{Lys}$ priming is shown. Annealing reaction mixtures contained either BSA (lanes a and b), the RNA binding protein QKI-6 (lane c), 16S rRNA (lanes d and f), or hA3G (lanes e and f). tRNA$_3^{Lys}$ priming was carried out using deproteinized annealed complexes.

tRNA$_3^{Lys}$ priming. We have previously reported that the effect of NCp7 on the tRNA$_3^{Lys}$/viral RNA annealing configuration is retained even after NCp7 is removed (10), and one can thus see the increase in priming with increased amounts of NCp7, whether NCp7 is left in the reaction mixture (lanes b and c) or not (lanes d and e).

Figure 1B shows the effect of adding hA3G during annealing. tRNA$_3^{Lys}$ was first annealed to viral RNA with NCp7 in the absence or presence of hA3G, with BSA present when hA3G was absent. The annealed complex was used in the reverse transcription reaction in the presence of these proteins (lanes a and b) or was first deproteinized before use in the reverse transcription reaction (lanes c and d). In either case, the prior presence of hA3G during annealing can be seen to inhibit tRNA$_3^{Lys}$ priming. However, the initiation of reverse transcription is much stronger when a deproteinized primer/template is used.

In Fig. 1C, we show that while hA3G inhibits tRNA$_3^{Lys}$ priming (lane f), the presence of another RNA binding protein, QKI-6 (34) (lane c), has no effect on tRNA$_3^{Lys}$ priming, making it less likely that hA3G inhibits tRNA$_3^{Lys}$ priming by sterically blocking the tRNA$_3^{Lys}$-viral RNA interaction. The presence of a nonspecific RNA such as bacterial 16S rRNA also had no inhibitory effect upon tRNA$_3^{Lys}$ priming (lane d), nor did its presence prevent the inhibition of tRNA$_3^{Lys}$ priming by hA3G (lanes e and f), suggesting that nonspecific RNA will not sequester hA3G and prevent its inhibition of tRNA$_3^{Lys}$ priming.

The hA3G-induced inhibition of tRNA$_3^{Lys}$ priming is associated with an inhibition of tRNA$_3^{Lys}$ annealing to viral RNA. tRNA$_3^{Lys}$ annealing to viral RNA was measured in two ways. One way measures the ability of tRNA$_3^{Lys}$, 3′ end labeled with ^{32}P, to bind to synthetic viral genomic RNA, as facilitated by NCp7. The free tRNA$_3^{Lys}$ is separated from the tRNA$_3^{Lys}$/viral RNA complex by electrophoresis. This electrophoretic band shift assay is shown in Fig. 2A. Lane 1 shows the mobility of free tRNA$_3^{Lys}$, while the remaining lanes (2 to 7) represent reactions in which viral RNA is also present and show both free tRNA$_3^{Lys}$ and the shifted band representing the tRNA$_3^{Lys}$/viral RNA complex. These lanes represent annealing reaction mixtures in which additional components have been added, such as BSA (lanes 1 and 2) 16S rRNA (lanes 4 and 6), the RNA binding protein QKI-6 (34) (lane 3), and hA3G (lanes 5 and 6). The ratio of annealed tRNA$_3^{Lys}$ to free tRNA$_3^{Lys}$ is shown below each lane and indicates that only hA3G inhibits annealing, and it does so by approximately 50%. As was shown for inhibition of tRNA$_3^{Lys}$ priming, the inhibition of tRNA$_3^{Lys}$ annealing by hA3G appears to be specific, i.e., the RNA binding protein QKI-6 does not inhibit annealing by sterically blocking the tRNA$_3^{Lys}$-viral RNA interaction (lane 3). 16S rRNA alone does not inhibit annealing (lane 4), nor does it lessen the ability of hA3G to inhibit annealing (lane 6). There is a small amount of tRNA$_3^{Lys}$ (11%) that is annealed to viral RNA even in the absence of NCp7 (lane 7). It is not clear if this tRNA$_3^{Lys}$ can initiate reverse transcription, since no tRNA$_3^{Lys}$ priming was detected in the absence of NCp7 in the annealing reaction (Fig. 1A and C, lanes a).

In Fig. 2B, the same experimental strategy was used, but the tRNA$_3^{Lys}$ primer was replaced with an 18-nt DNA primer complementary to the PBS and was 5′ end labeled with ^{32}P. It can be seen that hA3G (as well as 16S rRNA and the QKI-6
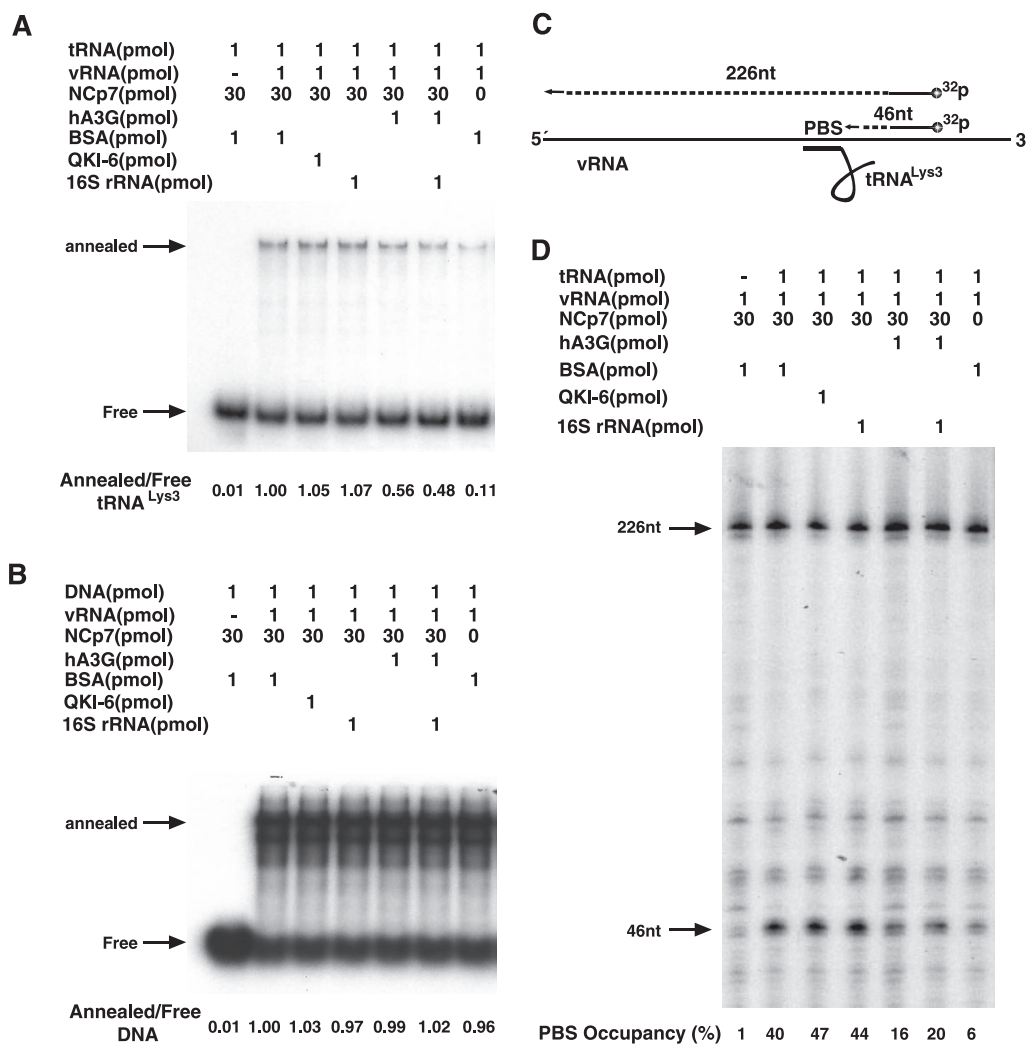
FIG. 2. Inhibition of NCp7-facilitated tRNA$_3^{Lys}$ annealing to viral RNA by hA3G. (A and B) Radioactive tRNA$_3^{Lys}$ (A) or a radioactive 18-nt DNA sequence (B) was annealed to synthetic viral RNA (vRNA), as facilitated by NCp7. The annealing reaction mixtures also contained either BSA, QKI-6, 16S rRNA, or hA3G. Free tRNA$_3^{Lys}$ or the DNA oligomer was separated from annealed complexes electrophoretically. The ratios of free tRNA$_3^{Lys}$ or DNA to viral RNA are listed below each lane. (C) Illustration showing the strategy used to measure the percentage of the PBSs occupied with tRNA$_3^{Lys}$ after tRNA$_3^{Lys}$ is annealed to synthetic viral RNA using NCp7. A 5'-^{32}P-end-labeled DNA primer annealed downstream of the PBS in viral RNA was extended with reverse transcription. The full-length extension product is 226 nt, while a truncated product, the extension of which is blocked by the presence of tRNA$_3^{Lys}$ on the PBS, is 46 nt. (D) Separation of the full-length and truncated extension products by 1D PAGE. The NCp7-facilitated annealing of tRNA$_3^{Lys}$ to viral RNA occurred in the presence of either BSA, QKI-6, 16S rRNA, or hA3G. The percentages of PBSs occupied by tRNA$_3^{Lys}$ are listed at the bottom of each lane, and they were determined by multiplying the ratio of truncated product to full-length product by 100.

RNA binding protein) has no effect on the DNA annealing. One reason for this may be the fact that while NCp7 is required for tRNA$_3^{Lys}$ annealing, it is not required for DNA annealing (lane 7). Since hA3G binds to both DNA and RNA (47), this suggests that hA3G may affect tRNA$_3^{Lys}$ annealing by binding to NCp7 and inhibiting its annealing function. This premise will be further investigated later in this paper.

While the electrophoretic band shift assay gives the relative degree of tRNA$_3^{Lys}$ annealing in the presence and absence of hA3G, we also have measured the fraction of PBSs occupied by tRNA$_3^{Lys}$ in the presence and absence of hA3G (Fig. 2C and D). The illustration in Fig. 2C shows the experimental strategy of the PBS occupancy assay, previously used by Beerens' and Berkhout's group (3). A ^{32}P-5'-end-labeled DNA oligomer is

annealed to sequences downstream of the PBS, using a synthetic viral RNA containing RU5 and leader sequences. The DNA primer is extended in an in vitro reverse transcription reaction to give a full-length product of 226 bases. If tRNA$_3^{Lys}$ is annealed to the PBS, it will block this extension and result in a shorter 46-base product. The 1D PAGE resolution of the RT extension products is shown in Fig. 2D, and the percentage of PBSs occupied by tRNA$_3^{Lys}$ is listed below the lanes. During extension of the DNA primer, there appears to be a series of pauses in reverse transcription, including one at the 46-base-long product, so that even with no tRNA$_3^{Lys}$ present, 1% of the PBS appears to be occupied (lane 1). In the absence of NCp7 in the annealing reaction (lane 7), approximately 6% of the PBS is occupied, supporting the conclusion from the data
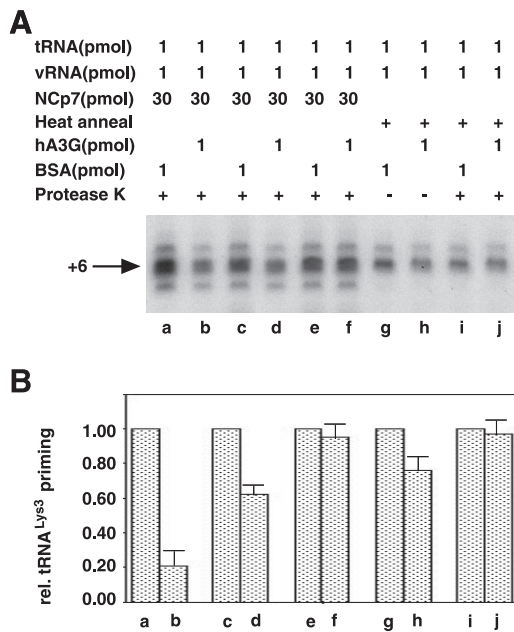
A

tRNA(pmol)	1	1	1	1	1	1	1	1	1	1
vRNA(pmol)	1	1	1	1	1	1	1	1	1	1
NCp7(pmol)	30	30	30	30	30	30				
Heat anneal							+	+	+	+
hA3G(pmol)		1		1		1		1		1
BSA(pmol)	1		1		1		1		1	
Protease K	+	+	+	+	+	+	-	-	+	+

+6 →

a b c d e f g h i j

B

FIG. 3. Effect of the order of addition of reactants upon tRNA$_3^{Lys}$ priming. (A) The radioactive tRNA$_3^{Lys}$ extended 6 bases by reverse transcription and resolved by 1D PAGE. (B) The quantitation of the gels shown in panel A, using the major middle band. Lanes a, c, e, g, and i represent reverse transcription reactions using annealed complexes (tRNA$_3^{Lys}$ annealed to viral RNA [vRNA]) exposed to BSA during their formation, while lanes b, d, f, h, and j represent reverse transcription reactions using annealed complexes exposed to hA3G during their formation. In all cases, after reverse transcription the reaction products were deproteinized, alcohol precipitated, and resolved by 1D PAGE. Lanes: a and b, annealed complexes formed in the presence of BSA (a) or hA3G (b), deproteinized, and used in the reverse transcription reaction; c and d, annealed complex formed, deproteinized, and used in the reverse transcription reaction in the presence of either BSA (c) or hA3G (d); e and f, annealed complex formed, deproteinized, and exposed to either BSA (e) or hA3G (f) for 90 min (the annealed complex was then deproteinized and used in the reverse transcription reaction); g and h, tRNA$_3^{Lys}$ heat annealed to viral RNA and then exposed to either BSA (g) or hA3G (h) for 90 min and used in reverse transcription reactions; i and j, tRNA$_3^{Lys}$ heat annealed to viral RNA and then exposed to either BSA (i) or hA3G (j) for 90 min, deproteinized, and used in the reverse transcription reaction.

shown in Fig. 2A that a small amount of tRNA^{Lys} is annealed to viral RNA even in the absence of NCp7. When annealing is carried out in the presence of either BSA (lane 2), the RNA binding protein QKI-6 (lane 3), or 16S rRNA (lane 4), PBS occupancy reached levels of 40, 47, and 44%, respectively. PBS occupancy is reduced by hA3G to 16% (lane 5) and 20% (lane 6) when annealing is carried out in the presence of both 16S rRNA and hA3G.

In summary, the data shown in Fig. 2 demonstrate that the hA3G-induced decrease in tRNA$_3^{Lys}$ priming shown in Fig. 1 is largely a result of the inhibition of the annealing of tRNA$_3^{Lys}$ to the viral RNA and that this inhibition is not produced by another RNA binding protein, QKI-6, and the hA3G-induced inhibition is not affected by the presence of a nonspecific RNA such as 16S rRNA.

Effect of the order of addition of reactants on tRNA$_3^{Lys}$ priming. Figure 3A shows the radioactive tRNA$_3^{Lys}$ extended by 6 bases and resolved by 1D PAGE, while Fig. 3B represents the quan-

titation of these gels using the major middle band and shows the tRNA$_3^{Lys}$ priming relative (rel.) to that obtained in the absence of hA3G. Lanes a, c, e, g, and i represent RT reactions using annealing complexes not exposed to hA3G during their formation (but exposed to a similar concentration of BSA), while lanes b, d, f, h, and j represent RT reactions using annealing complexes exposed to hA3G during their formation. In the RT reactions represented in lanes a and b, tRNA$_3^{Lys}$ was annealed to viral RNA with NCp7 for 90 min in the presence of either BSA (a) or hA3G (b). The reaction mixtures were then deproteinized with protease K and phenol-chloroform, and after ethanol precipitation the viral RNA pellet was resuspended and used in the RT priming reaction. It can be seen that exposure of the annealing reaction to hA3G resulted in an 80% inhibition of tRNA$_3^{Lys}$ priming. In lanes c and d, NCp7-facilitated annealing was done in the absence of hA3G, and, following deproteinization and ethanol precipitation, the RT reaction was run either in the absence (c) or presence (d) of hA3G. It can be seen that there is a 40% inhibition of tRNA$_3^{Lys}$ priming under these conditions. However, based on the results shown in lanes e and f, it is likely that this inhibition of tRNA$_3^{Lys}$ priming is not the result of inhibiting tRNA$_3^{Lys}$ annealing but rather affects a later step in tRNA$_3^{Lys}$ priming. Thus, in lanes e and f, the annealing complex is treated similarly to that in lanes c and d, but after a 90-min exposure of the tRNA$_3^{Lys}$/viral RNA complex to hA3G, another deproteinization and ethanol precipitation step occurs to remove hA3G before running the RT reaction. This results in only 10% inhibition and indicates that, once annealing of tRNA$_3^{Lys}$ to the viral RNA is finished, exposure of the annealed complex to hA3G does not affect tRNA$_3^{Lys}$ priming. The results obtained for paired lanes c and d as well as e and f are also obtained if heat is used instead of NCp7 to anneal tRNA$_3^{Lys}$ to viral RNA. Lanes g and h show that if hA3G is absent during annealing but present during the RT reaction, there is a 25% inhibition of priming, while if hA3G is removed before running the reaction (lanes i and j) there is very little inhibition of tRNA$_3^{Lys}$ priming.

Inhibition of tRNA$_3^{Lys}$ priming is dependent upon the amount of hA3G used and can be rescued with increasing amounts of NCp7. The results so far indicate that hA3G inhibition of tRNA$_3^{Lys}$ priming is occurring at the annealing stage. In lanes e to h in Fig. 4A, we see that the hA3G-facilitated inhibition of tRNA$_3^{Lys}$ priming is directly proportional to the amount of hA3G used. Lanes a to d show that tRNA$_3^{Lys}$ priming is not affected by increasing concentrations of BSA. On the other hand, the use of increasing amounts of NCp7 (Fig. 4B, lanes e to h) can overcome the inhibitory effect of hA3G on tRNA$_3^{Lys}$ priming. Increasing doses of NCp7 also will increase annealing in the absence of hA3G (lanes a to d), but because of the high level of initial annealing, the differences are much smaller. These data indicate that hA3G may prevent NCp7 from facilitating annealing by binding to NCp7. The alternative interpretation, that NCp7 prevents hA3G from binding to RNA and thereby sterically blocking annealing, seems less likely, since hA3G is unable to block NCp7-independent DNA annealing to viral RNA, as shown in Fig. 2B. Furthermore, the next set of experiments shows that the annealing of tRNA$_3^{Lys}$ by an NCp7 variant unable to bind to hA3G is insensitive to hA3G inhibition.
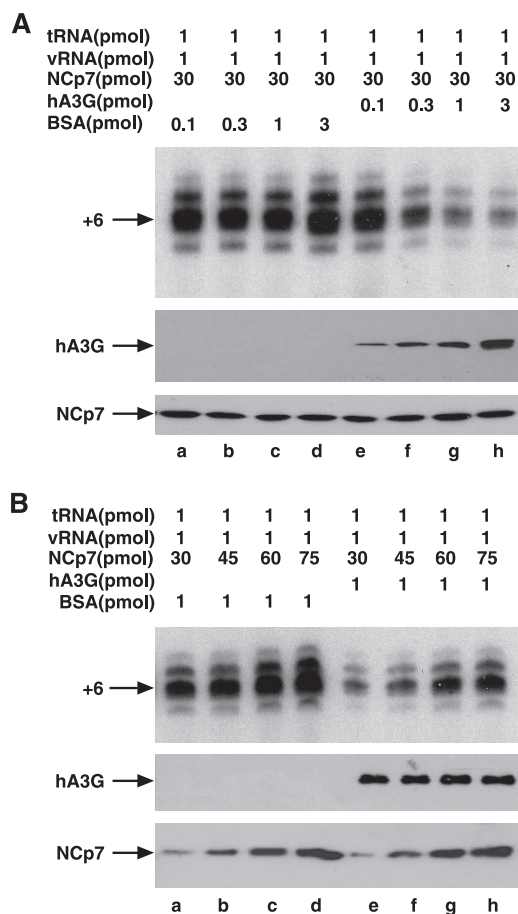
FIG. 4. Inhibition of tRNA$_3^{Lys}$ priming is dependent upon the amount of hA3G used and can be rescued with increasing amounts of NCp7. The effect of increasing concentrations of hA3G (A) or NCp7 (B) upon the ability of the annealed complex to initiate reverse transcription is shown. (A) The upper portion shows 1D PAGE patterns of tRNA$_3^{Lys}$ extended by 6 bases. The nucleocapsid concentration used for annealing was held constant. Lanes a to d, increasing concentrations of BSA; lanes e to h, increasing concentrations of hA3G. The middle and lower portions show Western blots of end reactions probed with either anti-hA3G or anti-NCp7. (B) The upper portion shows 1D PAGE patterns of tRNA$_3^{Lys}$ extended by 6 bases. Lanes a to f represent increasing amounts of NCp7 used for annealing. Lanes a to d, annealing reaction mixture exposed to BSA; lanes e to h, annealing reaction mixture exposed to hA3G. The middle and lower portions show Western blots of end reactions probed with either anti-hA3G or anti-NCp7. vRNA, viral RNA.

hA3G-facilitated inhibition of tRNA$_3^{Lys}$ priming requires an hA3G-NCp7 interaction. Figure 5A shows the sequence of wild-type and mutant nucleocapsid proteins used in the next experiments. Mutants b and c have the five basic amino acids changed to either alanines or glycines, respectively. Mutant d has the three cysteines in each zinc finger changed to alanines, while mutant e has had the aromatic amino acids F16 and W37 in the first and second zinc fingers, respectively, replaced with alanines. Mutant f has had the four basic amino acids in the linker region between the two zinc fingers changed to alanines.

For Fig. 5B, wild-type and mutant NCp7s were incubated with hA3G, and their ability to be coimmunoprecipitated with anti-hA3G was detected on Western blots probed with anti-

NCp7. It can be seen that the main NCp7 species interacting with hA3G are the wild type and mutant e, although a very small amount of interaction can be detected with NCp7 mutant f. It has been suggested that this interaction is facilitated by RNA (31, 42, 50), which is consistent with the fact that three of the four noninteracting NCp7 mutants have lost basic amino acid sequences in the leader (b and c) or linker (f) region. For the experiments shown in Fig. 5C, RNase A was added to hA3G and wild-type NCp7 either before (lane b) or after (lane c) their mixing. Western blots of the coimmunoprecipitates show that the exposure to RNase A severely reduces the interaction between hA3G and NCp7 (lane b) and that RNA is required to maintain this interaction (lane c).

We next measured tRNA$_3^{Lys}$ priming from tRNA$_3^{Lys}$ annealed to viral RNA with wild-type or mutant NCp7 in the presence or absence of hA3G. The electrophoretic results are shown in Fig. 6A. Lanes a to f and lanes a′ to f′ represent the wild-type and mutant NCp7 species (shown in Fig. 5A) used to anneal tRNA$_3^{Lys}$ to viral RNA in the absence (a to f) or presence (a′ to f′) of hA3G. The major band in each lane is quantitated in Fig. 6B and C. Figure 6B quantitates the tRNA$_3^{Lys}$ priming from complexes produced in the absence of hA3G by the different NCp7 mutants relative to that of wild-type NCp7. It has previously been reported that the basic amino acids flanking the first zinc finger are most important for the tRNA$_3^{Lys}$ annealing function of NCp7, with the zinc fingers playing a much smaller role (9, 13, 33). This can be seen in Fig. 6B, where NCp7 mutants missing the N-terminal basic amino acids (mutants shown in lanes b and c) or the linker basic amino acids (f) show tRNA$_3^{Lys}$ priming reduced to 10 or 20%, respectively, of that obtained with wild-type NCp7. NCp7 mutant d, with extensive mutations in both zinc fingers (AAHA/AAHA), does appear to have somewhat less ability to anneal tRNA$_3^{Lys}$ to viral RNA, since this annealed complex produces 70% of the tRNA$_3^{Lys}$ priming produced from the annealed complex formed using wild-type NCp7.

In Fig. 6C, we have compared the sensitivity to hA3G of tRNA$_3^{Lys}$ priming from annealed complexes produced by each type of NCp7. The levels of hA3G inhibition of tRNA$_3^{Lys}$ priming from each type of annealing complex compared to that of tRNA$_3^{Lys}$ priming in the absence of hA3G are as follows: lane a, 70%; lane b, 3%; lane c, 5%; lane d, 8%; lane e, 55%; and lane f, 20%. Of particular interest are the NCp7 species that are mutated in the zinc fingers (d and e). These produce complexes with tRNA$_3^{Lys}$ priming approximately 70% and 80% as active as complexes produced from wild-type NCp7 (Fig. 6B) but show very different sensitivities to inhibition by hA3G. Mutant d has all three cysteines in each zinc finger mutated to alanines, and it produces annealing complexes relatively insensitive (8%) to hA3G inhibition, while mutant e, for which phenylalanine and tryptophan in the first and second zinc fingers, respectively, were replaced with alanines, shows a 55% inhibition of tRNA$_3^{Lys}$ priming. Figure 5B showed that NCp7 mutant d does not bind to hA3G, while NCp7 e mutant does. There is thus a direct correlation between the ability of hA3G to inhibit tRNA$_3^{Lys}$ priming and its ability to bind to NCp7. These data therefore indicate that the inhibition of tRNA$_3^{Lys}$ priming is not due to the blocking of tRNA$_3^{Lys}$ annealing to viral RNA by hA3G bound to these RNA species but to the
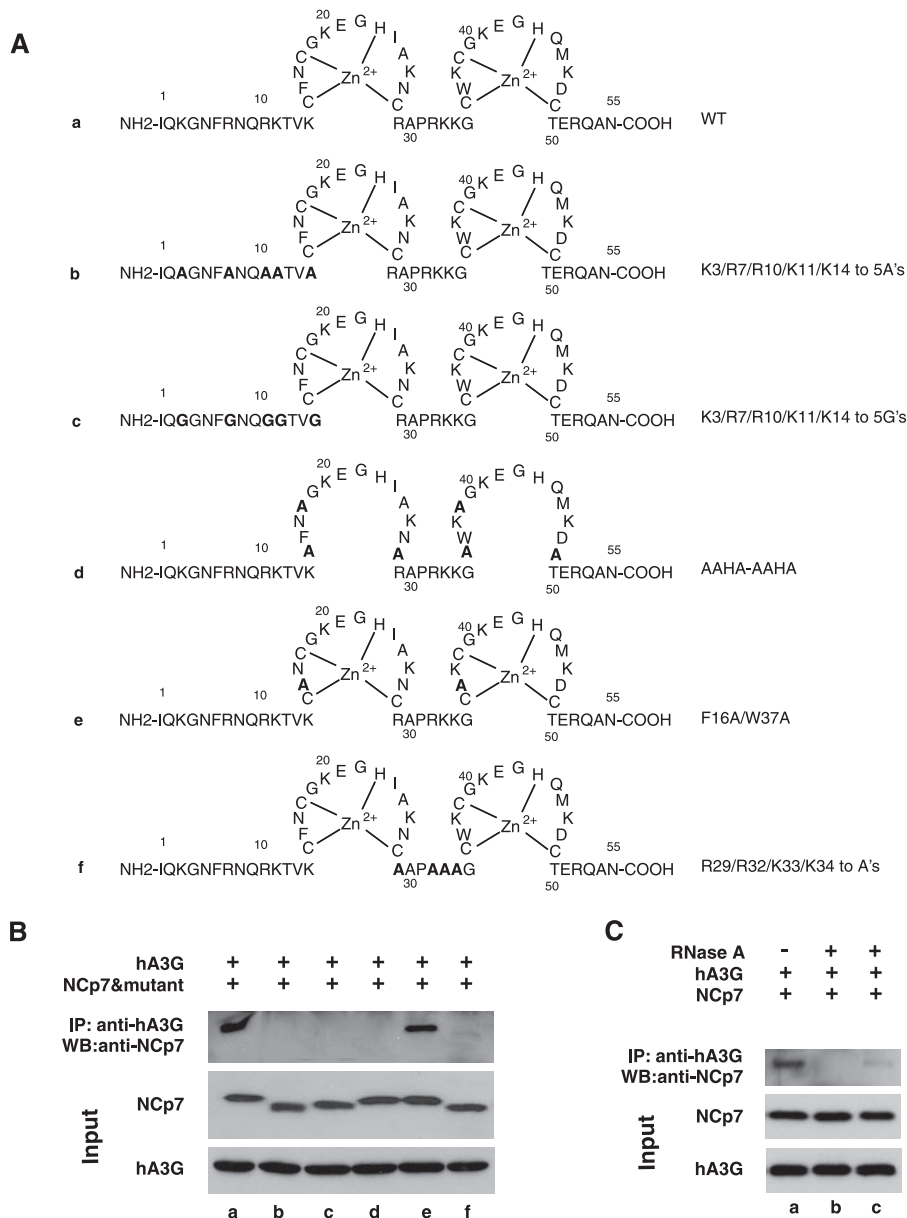
FIG. 5. Interaction between NCp7 and hA3G. (A) Sequences of wild-type and mutant nucleocapsids are shown. Sequences: a, wild type; b and c, the N-terminal five basic amino acids replaced with either alanine (b) or glycine (c); d, the three cysteines in each zinc finger replaced with alanines; e, F16 and W37 in the first and second zinc fingers, respectively, replaced with alanines; f, four basic amino acids in the linker region between the two zinc fingers replaced with alanine. (B) For the experiment shown in the upper portion, wild-type or mutant NCp7 was incubated with hA3G, and its ability to be coimmunoprecipitated with anti-hA3G was detected by Western blots (WB) probed with anti-NCp7. The middle and lower portions show Western blots of input reactions probed with either anti-NCp7 or anti-hA3G. (C) Role of RNA in the interaction between wild-type NCp7 and hA3G. The upper portion shows coimmunoprecipitation experiments that were performed similarly to those shown in panel B, except that for lanes b and c, RNase A was added to hA3G and wild-type NCp7 before (b) or after (c) their mixing. The middle and lower portions show Western blots of input reactions probed with either anti-NCp7 or anti-hA3G. IP, immunoprecipitation.

DISCUSSION

We have previously reported that when Vif-negative HIV-1 containing hA3G infects cells, there is a 55% reduction in the production of minus-strand strong-stop DNA compared to that obtained with virions lacking hA3G, and that this reduction is correlated with a similar reduction in the ability of $tRNA_3^{Lys}$ to initiate reverse transcription (19). To more clearly understand how hA3G inhibits $tRNA_3^{Lys}$ priming, we have studied this phenomenon in an in vitro reverse transcription system in which the primer $tRNA_3^{Lys}$/viral RNA template complex is produced by the NCp7-facilitated annealing of purified human $tRNA_3^{Lys}$ to synthetic viral RNA in the presence or absence of hA3G. Our results
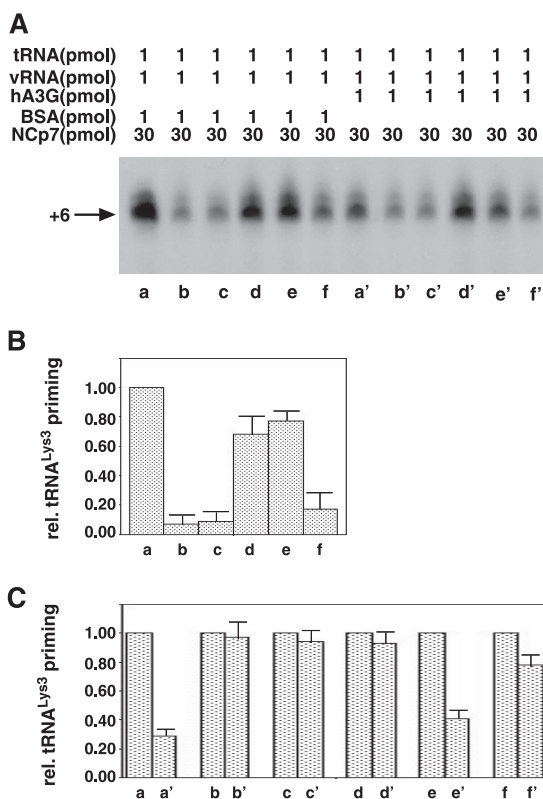
inhibition of NCp7-facilitated annealing through the binding of hA3G to NCp7.

A

tRNA(pmol)	1	1	1	1	1	1	1	1	1	1	1	1
vRNA(pmol)	1	1	1	1	1	1	1	1	1	1	1	1
hA3G(pmol)							1	1	1	1	1	1
BSA(pmol)	1	1	1	1	1	1						
NCp7(pmol)	30	30	30	30	30	30	30	30	30	30	30	30

+6 →

a b c d e f a' b' c' d' e' f'

B

C

FIG. 6. hA3G-facilitated inhibition of tRNA$_3^{Lys}$ priming requires an interaction between hA3G and NCp7. (A) 1D PAGE of tRNA$_3^{Lys}$ extended by 6 bases in an in vitro reverse transcription system, described in the legend to Fig. 1. Lanes a to f and lanes a' to f' represent the wild-type and mutant NCp7 species (shown in Fig. 5A) used to anneal tRNA$_3^{Lys}$ to viral RNA in the absence (a to f) or presence (a' to f') of hA3G. (B and C) The major band in each lane was quantitated by phosphorimaging. (B) tRNA$_3^{Lys}$ priming in the absence of hA3G relative (rel.) to tRNA$_3^{Lys}$ priming from the annealed complex produced with wild-type NCp7. (C) Comparison of tRNA$_3^{Lys}$ priming produced from each type of annealed complex in the presence of hA3G to that in its absence. vRNA, viral RNA.

show that hA3G inhibits tRNA$_3^{Lys}$ priming 70 to 80% compared to the level of priming in the absence of hA3G. hA3G must be present during the annealing process, as we have shown that hA3G will not disrupt the annealed complex once it is formed.

Data shown in Fig. 2 indicate that a significant part of this reduction in the initiation of reverse transcription (i.e., tRNA$_3^{Lys}$ priming) is due to an inhibition of annealing of tRNA$_3^{Lys}$ to the viral RNA. The hA3G-facilitated reduction in tRNA$_3^{Lys}$ annealing to viral RNA measured either by the electrophoretic band shift assay or by the PBS occupancy assay was 44 or 60%, respectively, somewhat less than the 70 to 80% decrease in tRNA$_3^{Lys}$ priming. This difference between the inhibition of annealing and priming could be due to the fact that the tRNA$_3^{Lys}$ that is annealed to viral RNA is not annealed correctly for optimum initiation of reverse transcription. For example, we have shown that in protease-negative virions, the tRNA$_3^{Lys}$ annealed by Gag has a reduced ability to initiate RT compared to that of an equal amount of tRNA$_3^{Lys}$ annealed in protease-positive virions that contain mature NCp7 (10).

Annealing of tRNA$_3^{Lys}$ to viral RNA is facilitated by nucleo-

capsid sequences, which can increase the rate of annealing in vitro up to fivefold (21). Both the mature NCp7 and these sequences in the precursor Gag protein will facilitate annealing (10). HIV-1 nucleocapsid has two zinc fingers. The basic amino acids flanking the N-terminal zinc finger are required for tRNA$_3^{Lys}$ annealing, but the two zinc fingers are not (9, 13, 22, 33). There are two known roles of NCp7 in the annealing process (21). There is a melting of a 4-bp helix predicted to be at the 5' region of the PBS (25), which may be facilitated by the zinc fingers, and there is the nucleation step that brings tRNA$_3^{Lys}$ and the PBS sequences together, which is probably facilitated primarily by the basic amino acids. A lack of effect upon the rate of annealing by mutations in the zinc fingers is explained by the fact that while the mutant NCp7 is a weaker duplex destabilizer, it is a better duplex-nucleating agent, and the two phenomena may cancel each other out (21). NCp7 appears to have a minimal effect on tRNA$_3^{Lys}$ structure, and annealing of the 4-base single-stranded region at the 3' terminus of the tRNA$_3^{Lys}$ to the 5' end of the PBS may result in an unzipping of other annealing regions in the tRNA$_3^{Lys}$ (22).

Two pieces of evidence indicate that the inhibition of tRNA$_3^{Lys}$ annealing to viral RNA by hA3G depends upon the ability of hA3G to interact with NCp7, and that this inhibition is not the result of a competition between hA3G and NCp7 for the annealing region. The replacement of three cysteines in each zinc finger of nucleocapsid with alanine (mutant d in Fig. 5A) still results in relatively strong tRNA$_3^{Lys}$ priming (Fig. 6A and B), but the mutant NCp7 does not interact with hA3G (Fig. 5B) and tRNA$_3^{Lys}$ priming is insensitive to hA3G (Fig. 6C). These data indicate that the intactness of one or both zinc fingers in nucleocapsid is required for interaction with hA3G and for the ability of hA3G to inhibit annealing. The other data suggesting that the hA3G-NCp7 interaction is responsible for inhibiting tRNA$_3^{Lys}$ annealing are shown in Fig. 2B, which demonstrates that the nucleocapsid-independent annealing of a DNA primer to viral RNA is not inhibited by hA3G. Although hA3G binds to both RNA and DNA (26, 27), both of these experiments show that hA3G does not sterically inhibit tRNA$_3^{Lys}$ annealing to viral RNA by competitively binding to viral RNA, since wild-type hA3G is present in both experiments.

The mechanism of binding of NCp7 to hA3G is not fully known. The hA3G-NCp7 interaction is RNA dependent, i.e., it is disrupted if the reaction solution containing NCp7 and hA3G is exposed to RNase A (Fig. 5C). The hA3G-NCp7 interaction probably also requires an ability of NCp7 to interact with RNA, since replacement of basic amino acids in the sequences flanking the first zinc finger of NCp7 (mutants b, c, and f in Fig. 3A) disrupts the hA3G-NCp7 interaction (Fig. 5B) and also disrupts the ability of NCp7 to facilitate tRNA$_3^{Lys}$ annealing to viral RNA (Fig. 6A and B). Since RNA cannot be detected in the purified NCp7 used here (R. J. Gorelick, unpublished data), the RNA involved is likely associated with the purified hA3G used. The nature of the RNA associated with hA3G is being investigated, and both Alu RNA (11) and 7SL RNA, a component of the host signal recognition particle (X.-F. Yu, personal communication), have been found to be associated with hA3G. It is not known, however, if the RNA serves as a bridge between NCp7 and hA3G or if RNA bound to hA3G more directly facilitates its binding with NCp7. This

latter phenomenon could result from an RNA-induced conformational change in hA3G that allows it to bind directly to NCp7. This might first involve an initial binding of hA3G-associated RNA with the basic amino acids flanking the first zinc finger in NCp7, which would then facilitate a direct protein interaction between hA3G sequences and the NCp7 zinc fingers required for this interaction.

It has been reported that HIV-1 produced from peripheral blood mononuclear cells has approximately 7 ± 4 molecules of hA3G/virion (46), while estimates of NCp7 molecules/virion have ranged from 1,400 (52) to 5,000 (5). Thus, the hA3G:NCp7 molar ratio in virions may be 0.001 to 0.005, while the in vitro system used here requires an hA3G:NCp7 molar ratio of 0.03, i.e., an hA3G:NCp7 ratio approximately 10 times greater than that found in the viruses produced from peripheral blood mononuclear cells. There are several possible explanations for this. First, we have found that the amount of hA3G required to inhibit $tRNA_3^{Lys}$ annealing in virions produced from normally permissive 293T cells transfected with hA3G is 10 times greater than that required for virions produced from the naturally nonpermissive H9 cells (19), and we suggest that other unknown factors may be present in the naturally nonpermissive cells to allow more efficient inhibition of $tRNA_3^{Lys}$ priming by hA3G. Any such unknown factors are not present in our in vitro reaction. Second, we may also consider the fact that the viral assembly stage at which $tRNA_3^{Lys}$ is annealed to viral RNA is not known. The select packaging of $tRNA_3^{Lys}$ into viruses may reflect an earlier assembly stage at which $tRNA_3^{Lys}$ is concentrated around a Gag/GagPol/viral RNA complex and in which annealing occurs. In fact, HIV-1 assembly stages of progressively increasing size have been detected (14). Work has also been reported that defines a $tRNA_3^{Lys}$ packaging/annealing complex consisting of Gag, GagPol, lysyl-tRNA synthetase, $tRNA^{Lys}$, and viral RNA (32), and this complex could represent an early assembly intermediate. It is, in fact, the nucleocapsid sequence in Gag, rather than mature NCp7, that probably is involved in the initial annealing of $tRNA_3^{Lys}$ (10). Therefore, in considering the inhibitory effect of hA3G on nucleocapsid-facilitated annealing of $tRNA_3^{Lys}$ to viral RNA, we might look at earlier assembly complexes with fewer Gag molecules than those found in the mature virion and also look for Gag molecules involved in annealing that might be distinguished from those that are not. Such molecules might be distinguished by their binding to GagPol, which is required for $tRNA_3^{Lys}$ annealing (10), by specific viral RNA sequences to which Gag nucleocapsid binds, such as the PBS or even the nearby Ψ RNA packaging sequence, or by the binding of Gag to lysyl-tRNA synthetase (32).

ACKNOWLEDGMENTS

REFERENCES

1. **Alce, T. M., and W. Popik.** 2004. APOBEC3G is incorporated into virus-like particles by a direct interaction with HIV-1 Gag nucleocapsid protein. J. Biol. Chem. **279:**34083–34086.
2. **Arts, E. J., X. Li, Z. Gu, L. Kleiman, M. A. Parniak, and M. A. Wainberg.** 1994. Comparison of deoxyoligonucleotide and tRNA(Lys-3) as primers in an endogenous human immunodeficiency virus-1 in vitro reverse transcription/template-switching reaction. J. Biol. Chem. **269:**14672–14680.
3. **Beerens, N., and B. Berkhout.** 2000. In vitro studies on tRNA annealing and reverse transcription with mutant HIV-1 RNA templates. J. Biol. Chem. **275:**15474–15481.
4. **Bishop, K. N., R. K. Holmes, and M. H. Malim.** 2006. Antiviral potency of APOBEC proteins does not correlate with cytidine deamination. J. Virol. **80:**8450–8458.
5. **Briggs, J. A., M. N. Simon, I. Gross, H. G. Krausslich, S. D. Fuller, V. M. Vogt, and M. C. Johnson.** 2004. The stoichiometry of Gag protein in HIV-1. Nat. Struct. Mol. Biol. **11:**672–675.
6. **Bruce, A. G., and O. C. Uhlenbeck.** 1978. Reactions at the termini of tRNA with T4 RNA ligase. Nucleic Acids Res. **5:**3665–3677.
7. **Carteau, S., R. J. Gorelick, and F. D. Bushman.** 1999. Coupled integration of human immunodeficiency virus type 1 cDNA ends by purified integrase in vitro: stimulation by the viral nucleocapsid protein. J. Virol. **73:**6670–6679.
8. **Cen, S., F. Guo, M. Niu, J. Saadatmand, J. Deflassieux, and L. Kleiman.** 2004. The interaction between HIV-1 Gag and APOBEC3G. J. Biol. Chem. **279:**33177–33184.
9. **Cen, S., Y. Huang, A. Khorchid, J. L. Darlix, M. A. Wainberg, and L. Kleiman.** 1999. The role of Pr55^{gag} in the annealing of tRNA$_3^{Lys}$ to human immunodeficiency virus type 1 genomic RNA. J. Virol. **73:**4485–4488.
10. **Cen, S., A. Khorchid, J. Gabor, L. Rong, M. A. Wainberg, and L. Kleiman.** 2000. Roles of Pr55^{gag} and NCp7 in tRNA$_3^{Lys}$ genomic placement and the initiation step of reverse transcription in human immunodeficiency virus type 1. J. Virol. **74:**10796–10800.
11. **Chiu, Y. L., H. E. Witkowska, S. C. Hall, M. Santiago, V. B. Soros, C. Esnault, T. Heidmann, and W. C. Greene.** 2006. High-molecular-mass APOBEC3G complexes restrict Alu retrotransposition. Proc. Natl. Acad. Sci. USA **103:**15588–15593.
12. **Cullen, B. R.** 2006. Role and mechanism of action of the APOBEC3 family of antiretroviral resistance factors. J. Virol. **80:**1067–1076.
13. **De Rocquigny, H., C. Gabus, A. Vincent, M.-C. Fournie-Zaluski, B. Roques, and J.-L. Darlix.** 1992. Viral RNA annealing activities of human immunodeficiency virus type 1 nucleocapsid protein require only peptide domains outside the zinc fingers. Proc. Natl. Acad. Sci. USA **89:**6472–6476.
14. **Dooher, J. E., and J. R. Lingappa.** 2004. Conservation of a stepwise, energy-sensitive pathway involving HP68 for assembly of primate lentivirus capsids in cells. J. Virol. **78:**1645–1656.
15. **Feng, Y. X., S. Campbell, D. Harvin, B. Ehresmann, C. Ehresmann, and A. Rein.** 1999. The human immunodeficiency virus type 1 Gag polyprotein has nucleic acid chaperone activity: possible role in dimerization of genomic RNA and placement of tRNA on the primer binding site. J. Virol. **73:**4251–4256.
16. **Fisher, A. G., B. Ensoli, L. Ivanoff, M. Chamberlain, S. Petteway, L. Ratner, R. C. Gallo, and F. Wong-Staal.** 1987. The sor gene of HIV-1 is required for efficient virus transmission in vitro. Science **237:**888–893.
17. **Gabuzda, D. H., K. Lawrence, E. Langhoff, E. Terwilliger, T. Dorfman, W. A. Haseltine, and J. Sodroski.** 1992. Role of Vif in replication of human immunodeficiency virus type 1 in CD4$^+$ T lymphocytes. J. Virol. **66:**6489–6495.
18. **Goncalves, J., Y. Korin, J. Zack, and D. Gabuzda.** 1996. Role of Vif in human immunodeficiency virus type 1 reverse transcription. J. Virol. **70:**8701–8709.
19. **Guo, F., S. Cen, M. Niu, J. Saadatmand, and L. Kleiman.** 2006. The inhibition of tRNA$_3^{Lys}$-primed reverse transcription by human APOBEC3G during human immunodeficiency virus type 1 replication. J. Virol. **80:**11710–11722.
20. **Guo, J., T. Wu, B. F. Kane, D. G. Johnson, L. E. Henderson, R. J. Gorelick, and J. G. Levin.** 2002. Subtle alterations of the native zinc finger structures have dramatic effects on the nucleic acid chaperone activity of human immunodeficiency virus type 1 nucleocapsid protein. J. Virol. **76:**4370–4378.
21. **Hargittai, M. R., R. J. Gorelick, I. Rouzina, and K. Musier-Forsyth.** 2004. Mechanistic insights into the kinetics of HIV-1 nucleocapsid protein-facilitated tRNA annealing to the primer binding site. J. Mol. Biol. **337:**951–968.
22. **Hargittai, M. R. S., A. Mangla, R. J. Gorelick, and K. Musier-Forsyth.** 2001. HIV-1 nucleocapsid protein zinc finger structures induce tRNA^{Lys3} tertiary structural changes, but are not critical for primer/template annealing. J. Mol. Biol. **312:**987–999.
23. **Harris, R. S., K. N. Bishop, A. M. Sheehy, H. M. Craig, S. K. Petersen-Mahrt, I. N. Watt, M. S. Neuberger, and M. H. Malim.** 2003. DNA deamination mediates innate immunity to retroviral infection. Cell **113:**803–809.
24. **Huang, Y., A. Shalom, Z. Li, J. Wang, J. Mak, M. A. Wainberg, and L. Kleiman.** 1996. Effects of modifying the tRNA$_3^{Lys}$ anticodon on the initiation of human immunodeficiency virus type 1 reverse transcription. J. Virol. **70:**4700–4706.

25. **Isel, C., C. Ehresmann, G. Keith, B. Ehresmann, and R. Marquet.** 1995. Initiation of reverse transcription of HIV-1: secondary structure of the HIV-1 RNA/tRNA^{Lys3} (template/primer) complex. J. Mol. Biol. **247:**236–250.

26. **Iwatani, Y., H. Takeuchi, K. Strebel, and J. G. Levin.** 2006. Biochemical activities of highly purified, catalytically active human APOBEC3G: correlation with antiviral effect. J. Virol. **80:**5992–6002.

27. **Jarmuz, A., A. Chester, J. Bayliss, J. Gisbourne, I. Dunham, J. Scott, and N. Navaratnam.** 2002. An anthropoid-specific locus of orphan C to U RNA-editing enzymes on chromosome 22. Genomics **79:**285–296.

28. **Jiang, M., J. Mak, A. Ladha, E. Cohen, M. Klein, B. Rovinski, and L. Kleiman.** 1993. Identification of tRNAs incorporated into wild-type and mutant human immunodeficiency virus type 1. J. Virol. **67:**3246–3253.

29. **Kaiser, S. M., and M. Emerman.** 2006. Uracil DNA glycosylase is dispensable for human immunodeficiency virus type 1 replication and does not contribute to the antiviral effects of the cytidine deaminase APOBEC3G. J. Virol. **80:**875–882.

30. **Kao, S., M. A. Khan, E. Miyagi, R. Plishka, A. Buckler-White, and K. Strebel.** 2003. The human immunodeficiency virus type 1 Vif protein reduces intracellular expression and inhibits packaging of APOBEC3G (CEM15), a cellular inhibitor of virus infectivity. J. Virol. **77:**11398–11407.

31. **Khan, M. A., S. Kao, E. Miyagi, H. Takeuchi, R. Goila-Gaur, C. Opi, C. L. Gipson, T. G. Parslow, H. Ly, and K. Strebel.** 2005. Viral RNA is required for the association of APOBEC3G with human immunodeficiency virus type 1 nucleoprotein complexes. J. Virol. **79:**5870–5874.

32. **Kleiman, L., R. Halwani, and H. Javanbakht.** 2004. The selective packaging and annealing of primer tRNALys3 in HIV-1. Curr. HIV Res. **2:**163–175.

33. **Lapadat-Tapolsky, M., C. Pernelle, C. Borie, and J.-L. Darlix.** 1995. Analysis of the nucleic acid annealing activities of nucleocapsid protein from HIV-1. Nucleic Acids Res. **23:**2434–2441.

34. **Larocque, D., and S. Richard.** 2005. QUAKING KH domain proteins as regulators of glial cell fate and myelination. RNA Biol. **2:**37–40.

35. **Lecossier, D., F. Bouchonnet, F. Clavel, and A. J. Hance.** 2003. Hypermutation of HIV-1 DNA in the absence of the Vif protein. Science **300:**1112.

36. **Li, J., M. J. Potash, and D. J. Volsky.** 2004. Functional domains of APOBEC3G required for antiviral activity. J. Cell Biochem. **92:**560–572.

37. **Madani, N., and D. Kabat.** 1998. An endogenous inhibitor of human immunodeficiency virus in human lymphocytes is overcome by the viral Vif protein. J. Virol. **72:**10251–10255.

38. **Mangeat, B., P. Turelli, G. Caron, M. Friedli, L. Perrin, and D. Trono.** 2003. Broad antiretroviral defence by human APOBEC3G through lethal editing of nascent reverse transcripts. Nature **424:**99–103.

39. **Mariani, R., D. Chen, B. Schrofelbauer, F. Navarro, R. Konig, B. Bollman, C. Munk, H. Nymark-McMahon, and N. R. Landau.** 2003. Species-specific exclusion of APOBEC3G from HIV-1 virions by Vif. Cell **114:**21–31.

40. **Mehle, A., B. Strack, P. Ancuta, C. Zhang, M. McPike, and D. Gabuzda.** 2004. Vif overcomes the innate antiviral activity of APOBEC3G by promoting its degradation in the ubiquitin-proteasome pathway. J. Biol. Chem. **279:**7792–7798.

41. **Newman, E. N., R. K. Holmes, H. M. Craig, K. C. Klein, J. R. Lingappa, M. H. Malim, and A. M. Sheehy.** 2005. Antiviral function of APOBEC3G can be dissociated from cytidine deaminase activity. Curr. Biol. **15:**166–170.

42. **Schäfer, A., H. P. Bogerd, and B. R. Cullen.** 2004. Specific packaging of APOBEC3G into HIV-1 virions is mediated by the nucleocapsid domain of the gag polyprotein precursor. Virology **328:**163–168.

43. **Sheehy, A. M., N. C. Gaddis, J. D. Choi, and M. H. Malim.** 2002. Isolation of a human gene that inhibits HIV-1 infection and is suppressed by the viral Vif protein. Nature **418:**646–650.

44. **Stopak, K., C. de Noronha, W. Yonemoto, and W. C. Greene.** 2003. HIV-1 Vif blocks the antiviral activity of APOBEC3G by impairing both its translation and intracellular stability. Mol. Cell **12:**591–601.

45. **Strebel, K., D. Daugherty, K. Clouse, D. Cohen, T. Folks, and M. A. Martin.** 1987. The HIV 'A' (sor) gene product is essential for virus infectivity. Nature **328:**728–730.

46. **Xu, H., E. Chertova, J. Chen, D. E. Ott, J. D. Roser, W. S. Hu, and V. K. Pathak.** 2007. Stoichiometry of the antiviral protein APOBEC3G in HIV-1 virions. Virology **360:**247–256.

47. **Yu, Q., R. Konig, S. Pillai, K. Chiles, M. Kearney, S. Palmer, D. Richman, J. M. Coffin, and N. R. Landau.** 2004. Single-strand specificity of APOBEC3G accounts for minus-strand deamination of the HIV genome. Nat. Struct. Mol. Biol. **11:**435–442.

48. **Yu, X., Y. Yu, B. Liu, K. Luo, W. Kong, P. Mao, and X. F. Yu.** 2003. Induction of APOBEC3G ubiquitination and degradation by an HIV-1 Vif-Cul5-SCF complex. Science **302:**1056–1060.

49. **Yu, X.-F.** 2006. Innate cellular defenses of APOBEC3 cytidine deaminases and viral counter-defenses. Curr. Opin. HIV AIDS **1:**187–193.

50. **Zennou, V., D. Perez-Caballero, H. Gottlinger, and P. D. Bieniasz.** 2004. APOBEC3G incorporation into human immunodeficiency virus type 1 particles. J. Virol. **78:**12058–12061.

51. **Zhang, H., B. Yang, R. J. Pomerantz, C. Zhang, S. C. Arunachalam, and L. Gao.** 2003. The cytidine deaminase CEM15 induces hypermutation in newly synthesized HIV-1 DNA. Nature **424:**94–98.

52. **Zhu, P., E. Chertova, J. Bess, Jr., J. D. Lifson, L. O. Arthur, J. Liu, K. A. Taylor, and K. H. Roux.** 2003. Electron tomography analysis of envelope glycoprotein trimers on HIV and simian immunodeficiency virus virions. Proc. Natl. Acad. Sci. USA **100:**15812–15817.